

## PHOTOPRODUCTION OF $\pi^0\pi^+$ ON THE PROTON AND DEUTERON AT $E_\gamma = 0.7 - 1.5$ GEV

A. MUSHKARENKOV<sup>1,2,\*</sup>, V. BELLINI<sup>3,4</sup>, J. P. BOCQUET<sup>5</sup>, L. CASANO<sup>5</sup>,  
 A. D'ANGELO<sup>6,5</sup>, R. DI SALVO<sup>6</sup>, A. FANTINI<sup>6,7</sup>, D. FRANCO<sup>6,7</sup>, G. GERVINO<sup>8</sup>,  
 F. GHIO<sup>9</sup>, G. GIARDINA<sup>4,10</sup>, B. GIROLAMI<sup>9</sup>, A. GIUSA<sup>3,4</sup>, A. IGNATOV<sup>2</sup>,  
 A. LAPIK<sup>2</sup>, P. LEVI SANDRI<sup>11</sup>, A. LLERES<sup>5</sup>, F. MAMMOLITI<sup>3,4</sup>,  
 G. MANDAGLIO<sup>4,10</sup>, M. MANGANARO<sup>4,10</sup>, D. MORICCIANI<sup>6</sup>, V. NEDOREZOV<sup>2</sup>,  
 C. RANDIERI<sup>3,4</sup>, D. REBREYEND<sup>5</sup>, N. RUDNEV<sup>2</sup>, G. RUSSO<sup>3,4</sup>,  
 C. SCHAEERF<sup>6,7</sup>, M. L. SPERDUTO<sup>3,4</sup>, M. C. SUTERA<sup>4</sup>,  
 A. TURINGE<sup>2</sup> and V. VEGNA<sup>6,7</sup>

<sup>1</sup>*Istituto Nazionale di Fisica Nucleare sezione di Pavia, Pavia 27100, Italy*

<sup>2</sup>*Institute for Nuclear Research, Moscow 117312, Russia*

<sup>3</sup>*Dipartimento di Fisica e Astronomia, Università di Catania, I-95123 Catania, Italy*

<sup>4</sup>*INFN, Sezione di Catania, I-95123 Catania, Italy*

<sup>5</sup>*LPSC, Université Joseph Fourier, CNRS/IN2P3,*

*Institut National Polytechnique de Grenoble, France*

<sup>6</sup>*INFN, Sezione di Roma "Tor Vergata", I-00133 Roma, Italy*

<sup>7</sup>*Dipartimento di Fisica, Università di Roma "Tor Vergata", I-00133 Roma, Italy*

<sup>8</sup>*Dipartimento di Fisica Sperimentale, Università di Torino,*

*and INFN - Sezione di Torino, I-00125 Torino, Italy*

<sup>9</sup>*Istituto Superiore di Sanità, I-00161 Roma,*

*and INFN - Sezione di Roma, I-00185 Roma, Italy*

<sup>10</sup>*Dipartimento di Fisica, Università di Messina, I-98166 Messina, Italy*

<sup>11</sup>*INFN-Laboratori Nazionali di Frascati, I-00044 Frascati, Italy*

\**mushkar@pv.infn.it*

†*mushkar@cpc.inr.ac.ru*

The preliminary results obtained by the GRAAL collaboration for the  $\pi^0\pi^+$  photoproduction on the free and quasi-free proton (deuteron) at  $E_\gamma = 0.7-1.5$  GeV are presented. The total cross section of the  $\gamma p \rightarrow \pi^0\pi^+n$  reaction and invariant mass spectra for the  $\pi^+\pi^0$ ,  $\pi^+n$  and  $\pi^0n$  systems are presented in the photon energy range from 0.7 to 1.5 GeV. These results are in good agreement with the  $2\pi$ -MAID calculations.

### 1. Introduction

Double pion photoproduction processes give the main contribution to the total photoabsorption cross section at  $E_\gamma = 0.7-1.5$  GeV. They provide new information on the cascade channels of the nucleon resonances decays, e.g.  $N^* \rightarrow (\Delta\pi, \rho N, \sigma N) \rightarrow \pi\pi N$ . This information can highlight resonances which are not seen in the  $\pi N$  or  $\eta N$  channels and brings additional constraints for the theoretical models of the nucleon.

The presence of the 3 hadrons in the final states complicates the theoretical study of the  $2\pi$  as compared with the single  $\eta$  and  $\pi$  photoproduction. Existing theoretical models<sup>1,2,3,4,5</sup> assume different reaction mechanisms, thus leading to the sizeable differences in the predicted values of the experimental observables. As an example, the two recent models published in<sup>4</sup> and<sup>5</sup> predict significantly different energy dependences for the total cross-sections of the  $\gamma p \rightarrow \pi^0 \pi^+ n$  channel at  $E_\gamma$  above 0.75 GeV. The first model describes the  $2\pi$  processes evaluating 20 Feynman diagrams and 9 nucleon resonances having a mass below 1.8 GeV and rated with a (almost) certain existence by Particle Data Group. As a result, the total cross-section values are in qualitative agreement with the existing experimental data. In the second model, a compound fit of the  $(\pi N, \gamma N) \rightarrow (\pi N, \pi \pi N)$  experimental data within a coupled-channels approach is performed. Its predictions for the total cross-sections of the  $2\pi$  channels considerably differ from the experimental values.

The  $\pi^0 \pi^+$  process on the proton has been experimentally studied using DAPHNE and TAPS detectors at MAMI<sup>6,7,8</sup> for  $E_\gamma$  below 0.8 GeV. These unpolarized measurements have been complemented in the work<sup>8</sup> with the helicity dependent cross-sections  $\sigma_{1/2}$  and  $\sigma_{3/2}$ , corresponding to the absorption of circularly polarized photons by longitudinally polarized nucleons with anti-parallel and parallel relative spin orientations, respectively. It has been found that the model<sup>3</sup> can well describe experimental data for  $\sigma_{3/2}$ , for which the processes  $\gamma p \rightarrow D_{13} \rightarrow (\pi \Delta, \rho^+ n) \rightarrow \pi^0 \pi^+ n$  are largely responsible, but fails to describe  $\sigma_{1/2}$  indicating non-resonant mechanisms of the reaction which are not fully accounted in the model.

In this article, the experimental investigation of the  $\pi^0 \pi^+$  channel is extended up to an incident photon energy of 1.5 GeV and to the quasi-free case, with a combined use of proton and deuteron targets.

## 2. Setup

The experiment was performed at the GRAAL facility<sup>9</sup> which uses a tagged photon beam with  $E_\gamma=500-1500$  MeV ( $\Delta E_\gamma=16$  MeV) obtained from the laser-induced Compton backscattering of storage ring electrons with an energy of 6 GeV.

The reaction products were detected by the large-acceptance ( $0.95 \times 4\pi$ ) LAGRAN $\gamma$ E detector (fig. 1), which allows the measure and the identification of the photon-interaction products with a low background.

The central part of the LAGRAN $\gamma$ E detector surrounds a cryogenic liquid-hydrogen or deuterium target, having a length of 6 cm and a diameter of 5 cm. It consists of two cylindrical proportional chambers (track detectors), a layer formed of 32 plastic counters (Barrel), and a high-resolution BGO ball detector.

Two planar proportional chambers, a double wall of plastic counters, and a shower detector cover the forward polar region ( $\theta \leq 25^\circ$ ). A scintillator-lead-scintillator sandwich is also installed to cover the backward polar region ( $\theta \geq 155^\circ$ ).

In addition, gamma-beam monitors are used to obtain an absolute measurement of the incident  $\gamma$ -flux.

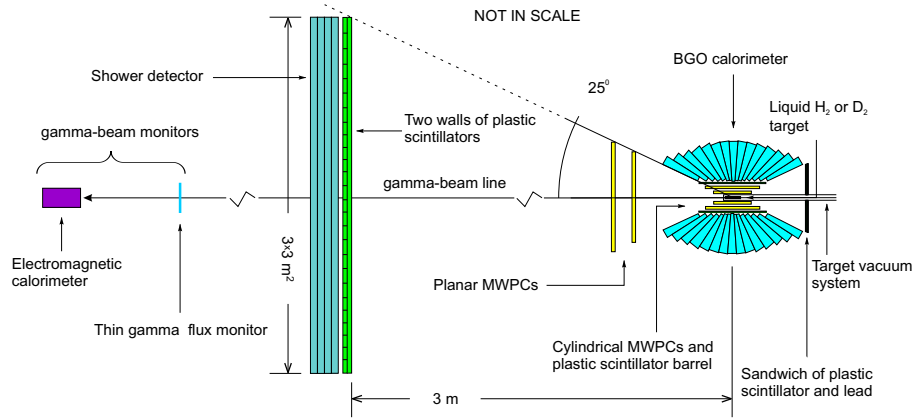


Fig. 1. Schematic view of the GRAAL detection system.

Detection efficiencies of the LAGRAN $\gamma$ E detector for charged particles and photons are  $\approx 70$ – $100\%$  depending on the software reconstruction conditions. Neutron detection efficiency amounts to  $\sim 60\%$  for the BGO ball<sup>10</sup> and  $\sim 22\%$  for the shower detector.<sup>11</sup>

### 3. Event Selection

Data collected on the proton and deuteron targets were analysed in a very similar way to select candidates of the  $\pi^0\pi^+$  photoproduction process. A signal from the tagging detector together with two photons of  $\pi^0$  decay in the BGO ball, as well as a neutron and  $\pi^+$  detected in the central or forward direction were required. Events with a two photons invariant mass within the range  $0.1$ – $0.18$  MeV were selected as those that containing a  $\pi^0$  in the final state (see fig. 2). In the central detection

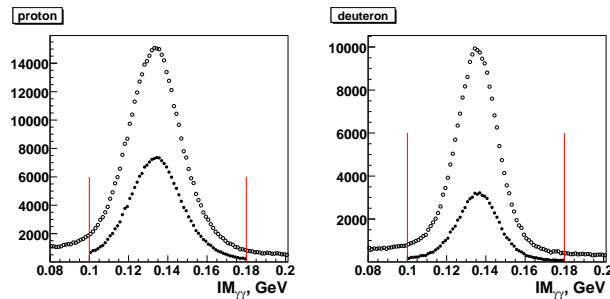


Fig. 2.  $2\gamma$  invariant mass distributions for selected  $\pi^0\pi^+$  events. The left (right) plot is from the proton (deuteron) target. Open and closed circles correspond to the data before and after the kinematical cuts applied, respectively. The vertical lines show the selected ranges.

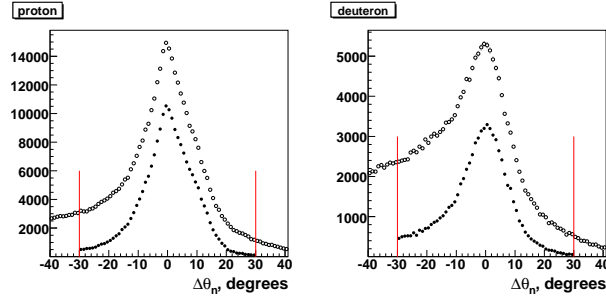
1200 *A. Mushkarenkov et al.*


Fig. 3. Differences between the calculated and measured neutron  $\theta$  angles for all selected events. Notations are the same as in fig. 2.

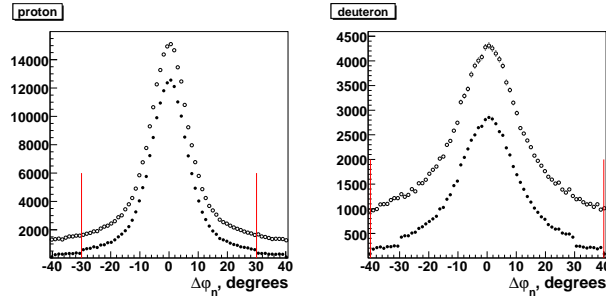


Fig. 4. Differences between the calculated and measured neutron  $\varphi$  angles for all selected events. Notations are the same as in fig. 2.

region,  $\pi^+$ s were identified from the analysis of the bidimensional  $\Delta E_{Barrel}$  vs  $\Delta E_{BGO}$  distribution. In the forward region, a  $\pi^+$  was required to be detected at least by both the planar proportional chambers and the double wall of plastic counters, under the condition that the measured time-of-flight (TOF) is  $\leq 11.5$  ns. The condition  $TOF \geq 12.5$  ns was instead required to identify neutrons detected in the forward direction by the shower detector. Furthermore, the measured energy and momentum of the  $\pi^0$  and the measured angles of the  $\pi^+$  and neutron provided, for each event, the necessary constraints for a 3-body kinematical fit that was performed to determine the unmeasured  $\pi^+$  and neutron energies. In addition, the following cuts were applied:  $30^\circ \leq \Delta\theta_n \leq 30^\circ$  and  $40^\circ \leq \Delta\varphi_n \leq 40^\circ$ , where  $\Delta\theta_n$  and  $\Delta\varphi_n$  are differences between measured and calculated polar and azimuthal angles, respectively (figs. 3 and 4).

A special attention was devoted to evaluate of the LAGRAN $\gamma$ E detector acceptance. The reaction  $\gamma p \rightarrow \pi^0 \pi^+ n$  was simulated using a uniform 3-body phase space distribution and analysed as the experimental data. Then, the simulated and detected events were compared in the bidimensional plot  $\theta_{\pi^0}$  vs  $T_{\pi^0}$  (see fig. 5), where  $\theta_{\pi^0}$  and  $T_{\pi^0}$  are the polar angle and kinetic energy of the  $\pi^0$  in the lab frame, respectively. In fig. 5 it can be clearly seen that  $\pi^0$  mesons with  $\theta \lesssim 20^\circ$

Photoproduction of  $\pi^0\pi^+$  on the Proton and Deuteron at  $E_\gamma = 0.7 - 1.5$  GeV 1201

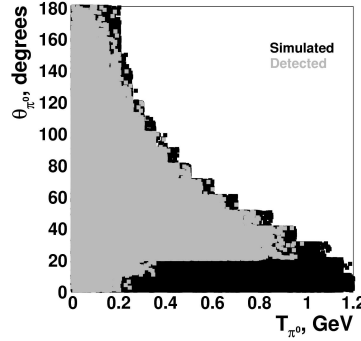


Fig. 5. The polar  $\pi^0$  angle as a function of its kinetic energy. Black points correspond to all simulated events, grey points correspond to simulated events that were accepted after the event selection procedure.

were not detected by our apparatus. This indicates that an extrapolation using a theoretical prediction is needed for the calculation of the total cross section.

#### 4. Invariant Mass Spertra

Fig. 6 shows a comparison of the invariant mass spectra for the  $\pi^0\pi^+$ ,  $\pi^0n$  and  $\pi^+n$  and

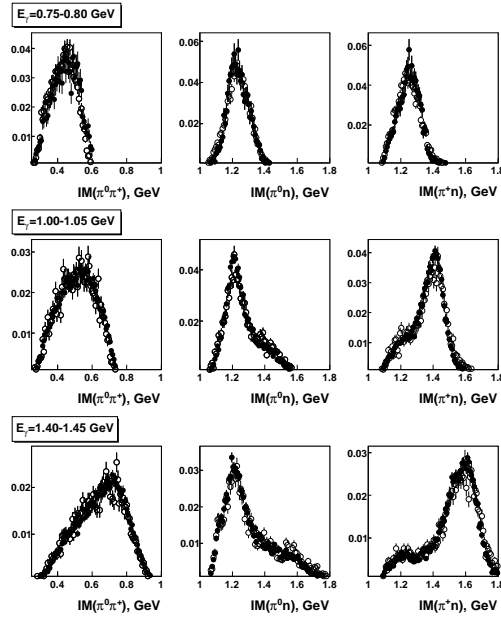


Fig. 6. The invariant mass spectra for the  $\pi^0\pi^+$ ,  $\pi^0n$  and  $\pi^+n$  systems for the 3 different  $E_\gamma$  energy range. Closed and open circles correspond to proton and deuteron targets, respectively.

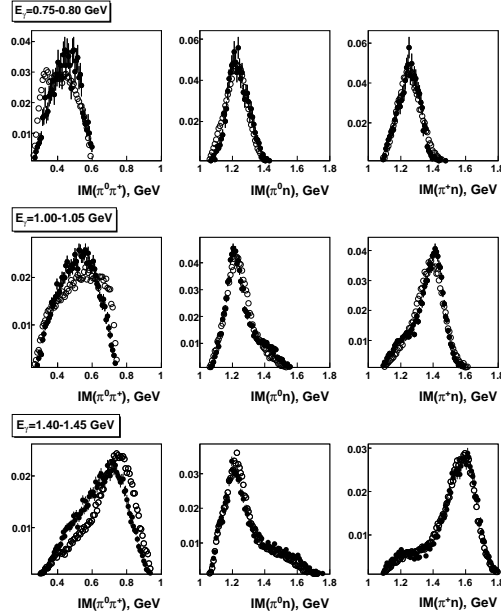
1202 *A. Mushkarenkov et al.*


Fig. 7. The invariant mass spectra for the  $\pi^0\pi^+$ ,  $\pi^0n$  and  $\pi^+n$  systems for the 3 different  $E_\gamma$  energy range. Closed and open circles correspond to experimental data on the proton and simulation, respectively.

$\pi^+n$  systems measured at the 3 different  $E_\gamma$  energy regions on the proton (closed circles) and deuteron (open circles) targets. The detector acceptance correction are not applied. No sizeable nuclear effects can be deduced from this comparison.

Fig. 7 shows a comparison between the experimental invariant mass spectra with the ones simulated using the GEANT3 code. In the simulation, the  $\pi^+\Delta^0$ ,  $\pi^0\Delta^+$ ,  $\rho^+n$  and  $\pi^0\pi^+n$  (with a uniform phase space distribution) intermediate mechanisms were implemented. The contribution of each partial channel was deduced from a fit of the total photoabsorption cross-section on the proton using a sum of 6 Breit-Wigner resonances plus a smooth non-resonant background.<sup>12</sup> The simulated data were analysed in the same way as the experimental one. It was found that this simple phenomenological model could fairly well describe the invariant mass spectra for both the  $\pi^0n$  and  $\pi^+n$  systems while the  $\pi^0\pi^+$  spectra indicate an slight model overestimation of the  $\rho^+n$  channel contribution. Due to its good agreement with the experimental data, this model was used to evaluate both the detection efficiency and the extrapolation correction of the data into the unmeasured kinematical region.

## 5. Total Cross-Section

The preliminary results of the total cross-section for the  $\gamma p \rightarrow \pi^0\pi^+n$  reaction are presented on the fig. 8. In this preliminary phase, only a relative normalization was evaluated for these data. The absolute normalization value was obtained by scaling

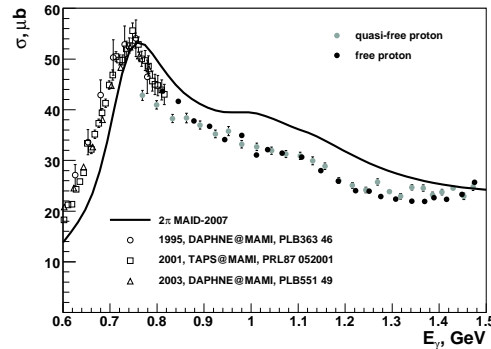


Fig. 8. The total cross-section of the reaction  $\gamma p \rightarrow \pi^0\pi^+n$ . The back and grey circles show the results of this work for the proton and deuteron targets, respectively. The open markers show the data previously obtained at MAMI.<sup>6,7,8</sup> The solid line shows  $2\pi$ -MAID calculation.<sup>4</sup>

to the total cross-section values obtained at MAMI. In fig. 8 the data that were thus obtained are compared with the  $2\pi$ -MAID model calculation.<sup>4</sup> One can see the model can well describe the basic trend of the observed data but there is a 5-10  $\mu\text{b}$  overestimation. Above 1.4 GeV there is an increase of the experimental data while the model still predicts a decreasing behaviour. According to the  $2\pi$ -MAID model, the peak at  $\sim 0.75$  GeV corresponds to the intermediate  $D_{13}(1520)$  resonance excitation and the broad bump centered at  $E_\gamma = 1-1.1$  GeV is due to the excitation of the  $F_{15}(1680)$  resonance and to the non-resonant  $\rho^+$  production. As it was said above, the obtained total cross-section values depend on the model selected for the detection efficiency calculation. Therefore, the detection efficiency calculation has to be done taking into account the some other different models that may provide us with a systematic error related to the model chosen.

## 6. Conclusion

Preliminary results on  $\pi^0\pi^+$  photoproduction on the proton and deuteron are presented in the photon energy range  $E_\gamma = 0.7-1.5$  GeV. The invariant mass spectra of the  $\pi^0n$  and  $\pi^+n$  system can be well described by a simple phenomenological model. For this reason, this model was used to evaluate both the detection efficiency and the extrapolation corrections, in order to evaluate the  $\pi^0\pi^+$  total cross section, which is in fairly good agreement with  $2\pi$ -MAID model. From the comparison between the obtained data and the predictions of the  $2\pi$ -MAID models, we can conclude that the main intermediate reaction mechanisms contributing to this channel are:  $\gamma + p \rightarrow D_{13}(F_{15}) \rightarrow \Delta^0\pi^+ \rightarrow \pi^0\pi^+n$ .

## Acknowledgments

This work was supported by Russian Foundation for Basic Research, grant no. 08-02-00646-a.

1204 *A. Mushkarenkov et al.*

## References

1. J. A. Gomez Tejedor and E. Oset, *Nucl. Phys. A* **600** (1996) 413.
2. K. Ochi, et al., *Phys. Rev. C* **56** (1997) 1472.
3. J. C. Nacher, et al., *Nucl. Phys. A* **695** (2001) 295.
4. A. Fix and H. Arenhovel, *Eur. Phys. J. A* **25** (2005) 115.
5. H. Kamano, et al., *arXiv:0909.1129.v1*.
6. A. Braghieri et al., *Phys. Lett. B* **363** (1995) 46.
7. W. Langgärtner et al., *Phys. Rev. Lett.* **87** (2001) 052001.
8. J. Ahrens et al., *Phys. Lett. B* **551** (2003) 49.
9. O. Bartalini et al., *Eur. Phys. J. A* **26** (2005) 399.
10. O. Bartalini et al., *Nucl. Inst. and Meth. A* **562** (2006) 85.
11. V. Kuznetsov et al., *Nucl. Instrum. Methods A* **487** (2002) 396.
12. N. Bianchi et al., *Phys. Rev. C* **54** (1996) 1688.